CONF-901116--14

DE91 001211

Photoion Auger-Electron Coincidence Measurements Near Threshold

J. C. Levin, C. Biedermann, N. Keller, L. Liljeby,[a] R. T. Short,[b] and I. A. Sellin

Department of Physics, University of Tennessee, Knoxville, Tennessee 37996-1200, USA
and Oak Ridge National Laboratory, Oak Ridge, Tennessee 37831-6377, USA

D. W. Lindle

National Institute of Standards and Technology, Gaithersburg, MD 20899, USA

The vacancy cascade which fills an atomic inner-shell hole is a complex process which can proceed by a variety of paths, often resulting in a broad distribution of photoion charge states. We have measured simplified argon photoion charge distributions by requiring a coincidence with a K-LL or K-LM Auger electron, following K excitation with synchrotron radiation, as a function of photon energy, and report here in detail the argon charge distributions coincident with K-L_1L_{23} Auger electrons. The distributions exhibit a much more pronounced photon-energy dependence than do the more complicated non-coincident spectra. Resonant excitation of the K electron to np levels, shakeoff of these np electrons by subsequent decay processes, double-Auger decay, and recapture of the K photoelectron through postcollision interaction occur with significant probability.

The development of synchrotron-radiation sources and modern x-ray optics has permitted studies of atomic inner shells with higher precision than previously possible. By energy selecting the radiation to a bandwidth on the order of the natural width of the atomic inner-shell hole state, it is possible to study details of the photoexcitation and subsequent autoionization processes as the inner-shell edge is probed very finely. Most such threshold studies have focused on measurements of photoelectron or Auger-electron spectra[1-3]. Valuable additional information can be gained by also examining charge distributions of photoions[4], which can be extracted and detected very efficiently by time-of-flight(TOF) spectrometers.

Many measurements of photoion charge distributions have been reported, including those conducted by Carlson, Krause, and coworkers using x-ray tubes and filters to photoionize inner shells of neon [5], argon [6], krypton [7], and xenon [8]. Tonuma, et al have measured the change in mean charge that occurs as the L edges of xenon are crossed.[9] We report here on the charge distributions of argon photoions as the K edge is probed very finely with synchrotron radiation. The broad distributions which follow the decay of a single K vacancy are due to the many radiative, Auger, and Coster-Kronig processes by which the atom relaxes to form a highly charged ion. We have measured photoions in coincidence with several of the Auger electrons by which the K vacancy is filled. The resultant photoion charge distributions are greatly simplified and reveal detailed information about the relaxation process.

The experiment was conducted on NIST beamline X-24A at NSLS and utilized both multibunch operations(for coincidence measurements) and single-bunch timing mode(for singles measurements). Details of the design[10] and performance[11] of the beamline have been discussed elsewhere. Synchrotron radiation was energy selected, to within $\approx$ 1 eV, by a double-crystal monochromator (containing Ge (111) crystals), and focused near the tip of a grounded stainless-steel gas jet. The needle was posi-

tioned in the extraction region of a TOF analyzer, and both were attached to an XYZ manipulator which permitted positioning of the needle in the source volume of a commercial cylindrical-mirror electron-energy analyzer. The TOF analyzer consisted of a series of field and drift regions of total length $\approx$ 5cm designed both to maintain space focusing and to restrict flight times of argon ions of all charge states to be less than the 550 ns bunch spacing characteristic of NSLS timing-mode operations. Photoions were detected by a pair of chevroned microchannel plates. Care was taken to assure uniform detection efficiency for all charge states; Ar^{q+} ions were accelerated in the last stage of the TOF analyzer to 2.4q keV kinetic energy. During timing-mode operations, photoions provided the start signal to a time-to-amplitude converter (TAC) which was stopped by a signal from the storage ring accompanying each burst of photons. In the coincidence measurements, the Auger-electron signal started the TAC, which was then stopped by the photoion signal. To obtain adequate coincidence rates, the cylindrical-mirror analyzer was operated in low-resolution (0.7% $\approx$ 20eV), non-retarding mode. Photoion peak widths were $\approx$ 2 ns, illustrating the resolution of the TOF spectrometer and associated electronics.

In order to study in detail ion yield as a function of photon energy in the vicinity of the K edge, it was necessary to monitor the energy calibration of the monochromator and to obtain a relative measure of photon flux through the source region. Both were achieved by bracketing each TOF spectrum with an absorption edge obtained by sweeping photon energy across the K-edge while recording the total argon-ion yield. The strong peak in the ion signal seen at the 1s-4p photoexcitation resonance 2.7 eV below the ionization threshold (3206.3 eV) served to calibrate absolute photon energy; all energies in this paper are referenced to this level.[12] The fitted area of this resonance was used to normalize each charge-state intensity to constant flux.

The singles TOF spectrum at the top of Fig. 1 was obtained during single bunch

operations with radiation tuned to the 4p resonance. As this resonance and the nearby absorption edge are traversed in small photon-energy increments, the mean argon photoion charge changes suddenly (Fig. 2), although there is relatively little evidence of structure. Somewhat more structure is evident when each charge state is examined individually (Fig. 3), although each charge state can be produced via several different decay paths.

The TOF spectra of Fig. 1 illustrate the simplification in charge distribution which results by requiring a coincidence with each of the three principal Auger lines, indicated in Fig. 1, by which a K vacancy can be filled. The broad singles spectrum represents an average of all possible radiative and nonradiative K-decay channels, with a small superimposed distribution resulting from decay of less-frequently created initial L or M vacancies. Although the Auger spectra are modified by the presence of the 4p satellite, diagram-line energies are shifted by only a few eV. The spectra obtained in coincidence with the K-$L_{23}L_{23}$ line at $\approx$ 2660 eV, K-L_1L_{23} at $\approx$ 2575 eV, and K-$L_{23}M_{23}$ at $\approx$ 2923 eV exhibit similarities to each other. Each consists of essentially three peaks; a weak high-charge-state peak, a strong central peak, and a lower-charge-state peak of intermediate intensity (note that Ar^{2+} is produced in coincidencr with K-$L_{23}M_{23}$ but is offscale in Fig. 1). The K-LL coincidence requirement ensures that each ion has two L-shell vacancies; each subsequent Auger or Coster-Kronig decay increases the ion charge by +1. Since L_{23} holes decay in argon with essentially unit probability via L-MM Auger decay,[13] and since L_1 holes decay through L_1–$L_{23}M$ Coster-Kronig transitions with probability 0.94[13], only the most intense, central 'diagram' peak in each coincidence spectrum is expected. The spectra of Fig. 1, obtained 2.7 eV below the K threshold at the 4p resonance, exhibit richer structure than this simple estimate suggests.

To understand in greater detail the origin of each of the three photoion charges

coincident with each Auger decay, we can examine, as a function of photon energy, the intensity of Ar^{4+}, Ar^{5+}, and Ar^{6+}, each normalized to constant photon flux, in the particular case of K-L_1L_{23} decay (Fig. 4). All three charge states exhibit a peak at the 1s-4p resonance; Ar^{4+} has a broad shoulder at slightly higher energy before diminishing asymptotically in intensity. In contrast, Ar^{5+} and Ar^{6+} continue to increase above threshold. These general characteristics are similar to those of Ar^{3+}, Ar^{4+}, and Ar^{5+} coincident with K-$L_{23}L_{23}$ decay (Fig.5), for which we have recently reported an analysis.[4] Most of the qualitative statements about charge state q coincident with K-$L_{23}L_{23}$ electrons made in [4] can be made about charge state q+1 coincident with K-L_1L_{23} Auger decay.

We have simulated the photoion distribution in the near-edge energy region by Monte-Carlo techniques. Four processes are important: excitation of the K electron to bound np levels, shakeoff of these resonantly populated np levels during subsequent steps in the vacancy cascade, double-Auger processes, and recapture of the K photoelectron above the K edge into bound Rydberg levels via post-collision interaction. We will briefly discuss the contribution of each process to production of Ar^{4+}, Ar^{5+}, and Ar^{6+} coincident with K-L_1L_{23} Auger decay. Further details are available elsewhere.[4]

By analogy to an earlier analysis of the argon K absorption edge[12], we can model the photon-energy dependence of Ar^{4+} in terms of resonant excitation of the K electron to bound np levels (Fig. 4), in which the peak energies have been constrained to be as previously measured. The fitted intensities obtained relative to that of 4p, $I(5p)+I(6p)+I(7p)=0.37\times I(4p)$, are lower than for the corresponding charge state, Ar^{3+}, coincident with K-$L_{23}L_{23}$, for which we find $I(5p)+I(6p)+I(7p)=0.47\times I(4p)$.[4] Both results are lower than the earlier absorption-edge measurement, $I(5p)+I(6p)+I(7p)=0.63\times I(4p)$.[12] This is a result of what can

be called Rydberg shakeoff of np electrons by subsequent Auger decays. In the K-$L_{23}L_{23}$ coincident case, there are two L-MM decays while the K-L_1L_{23} coincident data first experience an L_1-L_{23}M decay with probability 0.94 [13] prior to the two L-MM decays. The low-lying np electrons are removed by shielding changes and/or electron-electron correlation phenomena associated with the departure of an electron in L-MM or L-LM decay.

In the vicinity of the 4p resonance and below, virtually none of the K electrons is excited into the continuum. There are, nonetheless, substantial components of Ar^{5+} and Ar^{6+} produced. Two production mechanisms are responsible. The first is feeding of Ar^{5+} by Ar^{4+} through Rydberg shakeoff of the resonantly populated np levels as discussed above. Additional contributions to Ar^{5+} and Ar^{6+} arise from double Auger (L-MMM) processes, which have been measured to accompany L-MM decay, following L-shell ionization, with probability 9±1%.[14] Production of Ar^{5+} is thus seen to occur by different processes in different photon energy regimes, even in coincidence with a single Auger process, K-L_1L_{23}. Well above threshold, where the K photoelectron has no chance of being recaptured by post-collision interaction, Ar^{4+} follows straightforwardly from L-MM decay of two L_{23} holes following a single L_1-L_{23} decay. In the subthreshold energy region, more complicated excitation-autoionization or double-Auger processes are responsible.

There is a clear excess of Ar^{4+} in the photon energy region 2-7 eV above the 4p resonance similar to the excess of Ar^{3+} coincident with K-$L_{23}L_{23}$ decay. At these energies excitation of the K electron into the continuum becomes most probable, with an attendant increase in Ar^{5+} production. The phenomenon of post-collision interaction(PCI), in which the low-energy photoelectron transfers some of its energy to the higher-energy Auger electron, and is itself recaptured into a bound Rydberg level, is responsible for production of Ar^{4+} in this region. This effect has recently been

observed in the noncoincident yield of Ar^+ ions following L photoionization just above threshold[15] and has been explained by a fully quantum-mechanical treatment.[16] Unlike the K-$L_{23}L_{23}$ coincident data, for which Ar^{3+} production falls to near zero by $\approx$ 10 eV above the 4p resonance, Ar^{4+} falls to a non-zero asymptotic limit at this energy. This is due to L_1-MM decay which fills L_1 vacancies with probability $\approx$ 6%.

Coincidence measurements of argon photoions with Auger electrons result in simplified charge distributions which permit study of the photon-energy dependence of phenomena which are not accessible in singles data. Production of different charge states proceeds by quite distinct processes as does production of the same charge state in different energy regimes. Below threshold, resonant excitation to bound np levels, and frequent Rydberg shakeoff of these levels dominates. Far above threshold, energy-dependent shakeoff and double-Auger effects dominate. At intermediate energies, post-collision interaction provides the bridge resulting in a smooth transition between these regimes.[17]

This work was supported in part by NSF, and by USDOE under Contract DE-AC05-84OR21400 with Martin Marietta Energy Systems, Inc. We appreciate the technical support of Barry Karlin of NSLS, which is supported by USDOE under Contract DE-AC020-76CH00016.

Present address: [a]Manne Siegbahn Institute of Physics, S-10405 Stockholm, Sweden. [b]Analytical Chemistry Division, Oak Ridge National Laboratory, Oak Ridge, Tennessee.

REFERENCES

[1] A. Fahlman, M. O. Krause, T. A Carlson and A. Svensson, Phys. Rev. A **30**, 812 (1984).

[2] U. Becker, B. Langer, H. G. Kerkhoff, M. Kupsch, D. szostat, R. Wehlitz, P. A. Heimann, S. H. Liu, D. W. Lindle, T. A. Ferrett, and D. A. Shirley, Phys. Rev. Lett. **60**, 1490 (1988).

[3] M. O. Krause and C. D. Caldwell, Phys. Rev. Lett. **59**, 2736 (1987).

[4] J. C. Levin, C. Biedermann, N. Keller, L. Liljeby, R. T. Short, I. A. Sellin, and D. W. Lindle, Phys. Rev. Lett. **65**, 988 (1990).

[5] M. O. Krause, M. L. Vestal, and W. H. Johnston, Phys. Rev. **133**, A385 (1964).

[6] T. A. Carlson and M. O. Krause, Phys. Rev. **137**, A1655 (1965).

[7] M. O. Krause and T. A. Carlson, Phys. Rev. **158**, 18 (1967).

[8] T. A. Carlson, W. E. Hunt, and M. O. Krause, Phys. Rev. **151**, 41 (1966).

[9] T. Tonuma, A. Yagishita, H. Shibata, T. Koizumi, T. Matsuo, K. Shima, T. Mukoyama, and H. Tawara, J. Phys. B: At. Mol. Phys. **20**, L31 (1987).

[10] P. L. Cowan, S. Brennan, R. D. Deslattes, A. Henins, T.Jach, and E. G. Kessler, Nucl. Instrum. Methods **246**, 154 (1986).

[11] P. Cowan, S. Brennan, T. Jach, and D. W. Lindle, Rev. Sci. Instrum. **60**, 1603 (1989).

[12] M. Breinig, M. H. Chen, G. E. Ice, F. Parente, B. Crasemann, G. S. Brown, Phys. Rev. A **22**, 520 (1980).

[13] M. O. Krause, J. Phys. Chem. Ref. Data **8**, 307 (1979).

[14] T. A. Carlson and M. O. Krause, Phys. Rev. Lett. 17, 1079 (1966).

[15] W. Eberhardt, S. Bernstorff, H. W. Jochims, S. B. Whitfield, and B. Crasemann, Phys. Rev. A 38, 3808, (1988).

[16] J. Tulkki, T. Åberg, S. B. Whitfield, and B. Crasemann, Phys. Rev. A 41 181 (1990).

[17] G. B. Armen, T. Åberg, K. R. Karim, J. C., Levin, B. Crasemann, G. S. Brown, M. H. Chen, and G. E. Ice, Phys. Rev. Lett. 54, 182 (1985).

FIG. 1. Time-of-flight spectra for argon photoions produced using synchrotron radiation tuned to the 1s-4p resonance ≈2.7eV below the K-shell ionization threshold (≈ 3206.3eV). The last three spectra were measured in coincidence with the indicated Auger line. Although offscale on the bottom spectrum, Ar^{2+} is also produced coincident with K-$L_{23}M_{23}$ electrons, with intensity intermediate to that of Ar^{3+} and Ar^{4+}.

FIG. 2. Mean argon photoion charge in the vicinity of the 4p resonance.

FIG. 3. Charge fraction for argon photoions near the 4p resonance. Ar^{7+} is visible in the data but is omitted here for clarity.

FIG. 4. Top: Argon photoion yields coincident with Ar K-L_1L_{23} Auger electrons and normalized to constant photon flux as a function of photon energy relative to the 4p resonance. Bottom: Decomposition of Ar^{4+} into components resulting from excitation of the K electron into bound np levels. The shaded area results from recapture of the photoelectron through post-collision interaction or L_1-MM decay.

FIG. 5. Top: As in Fig. 4, but for Ar K-$L_{23}L_{23}$ Auger electrons. Bottom: As in Fig. 4 except that the shaded area results only from recapture of the photoelectron through post-collision interaction.

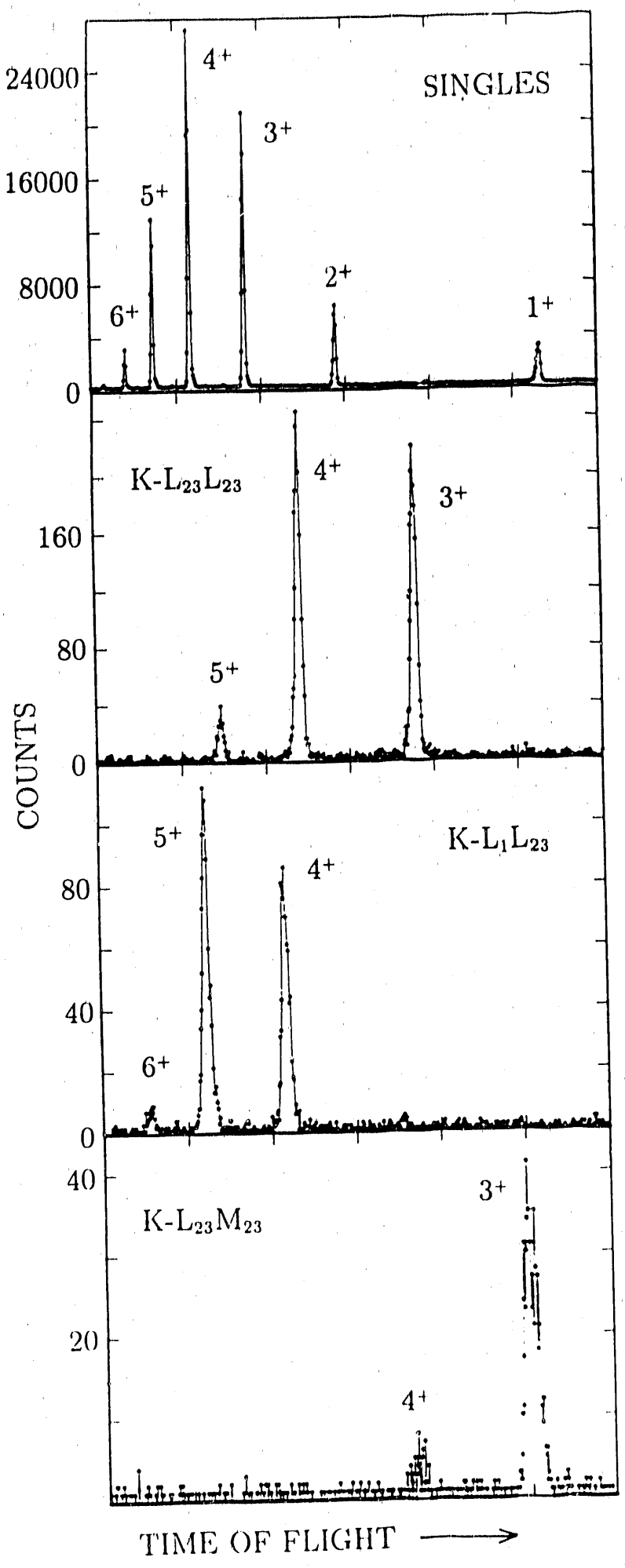
SINGLES
24000
16000
8000
0
6+
5+
4+
3+
2+
1+
K-L23L23
160
80
0
5+
4+
3+
K-L1L23
80
40
0
5+
4+
6+
K-L23M23
40
20
3+
4+
COUNTS
TIME OF FLIGHT

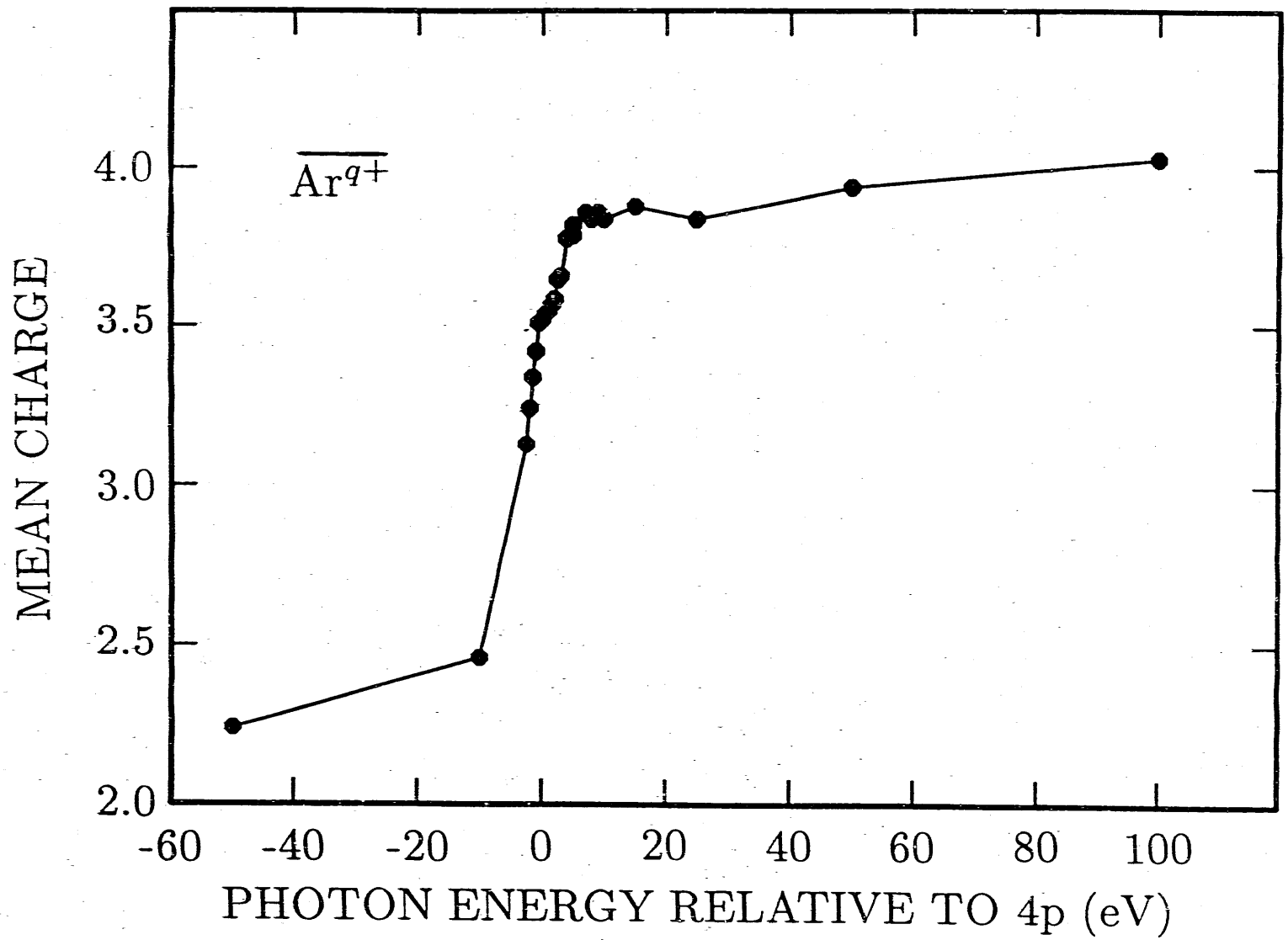
$\overline{Ar^{q+}}$
MEAN CHARGE
4.0
3.5
3.0
2.5
2.0
-60
-40
-20
0
20
40
60
80
100
PHOTON ENERGY RELATIVE TO 4p (eV)

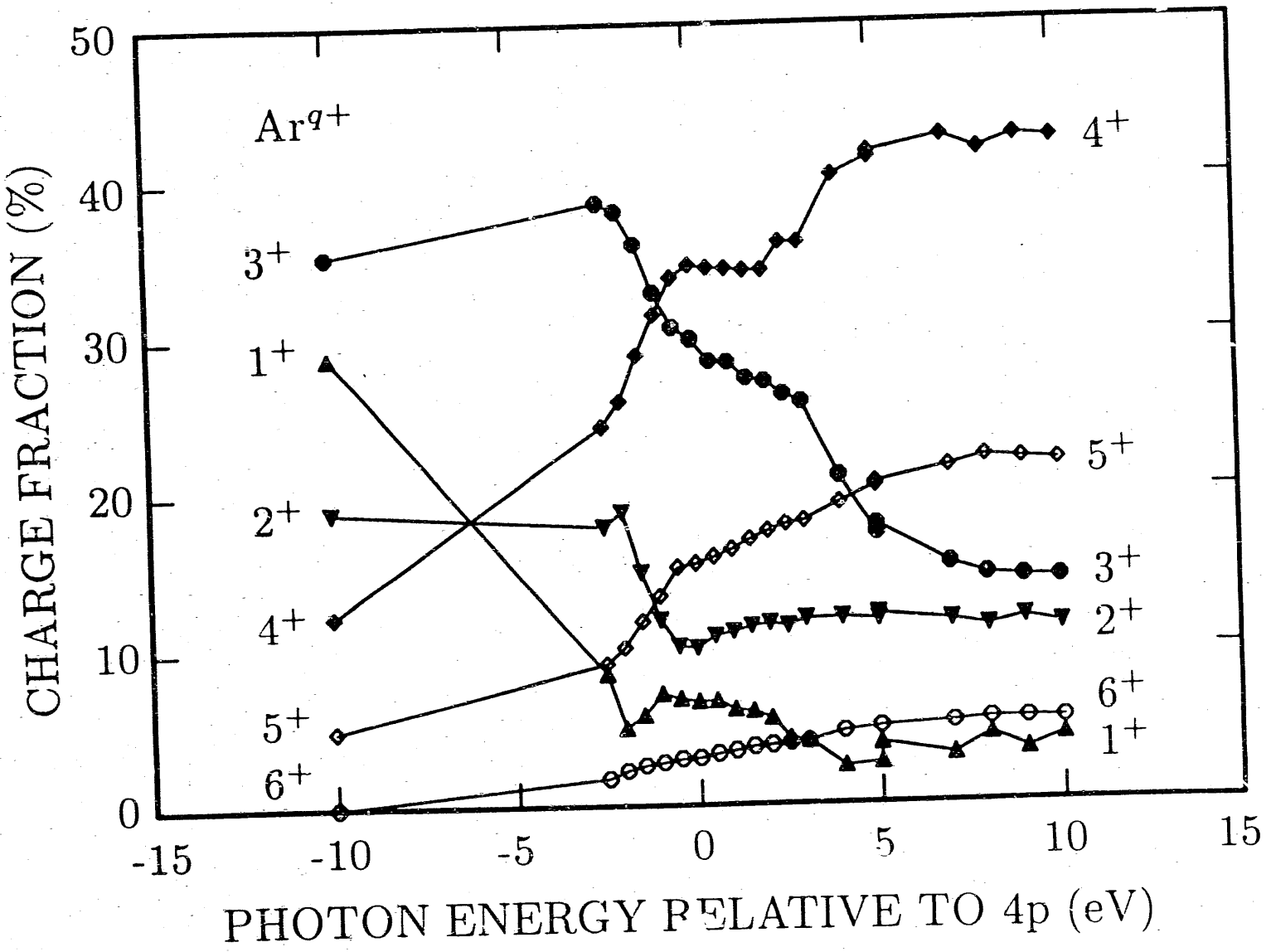
Ar^{q+}
CHARGE FRACTION (%)
PHOTON ENERGY RELATIVE TO 4p (eV)
50
40
30
20
10
0
-15
-10
-5
0
5
10
15
3+
1+
2+
4+
5+
6+
4+
5+
3+
2+
6+
1+

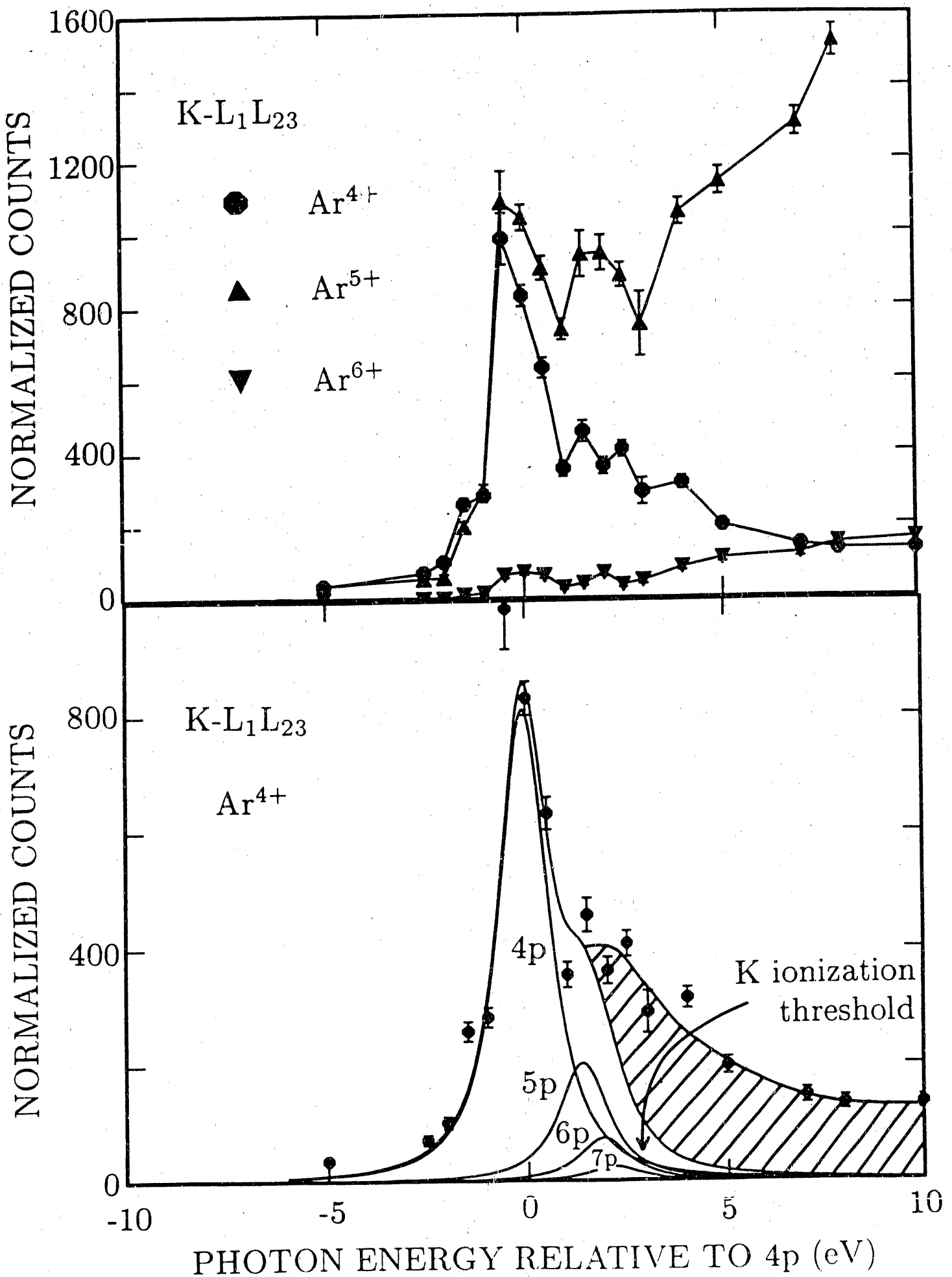
1600
1200
800
400
0
NORMALIZED COUNTS
K-L1L23
Ar4+
Ar5+
Ar6+
800
400
0
NORMALIZED COUNTS
K-L1L23
Ar4+
4p
5p
6p
7p
K ionization threshold
-10
-5
0
5
10
PHOTON ENERGY RELATIVE TO 4p (eV)

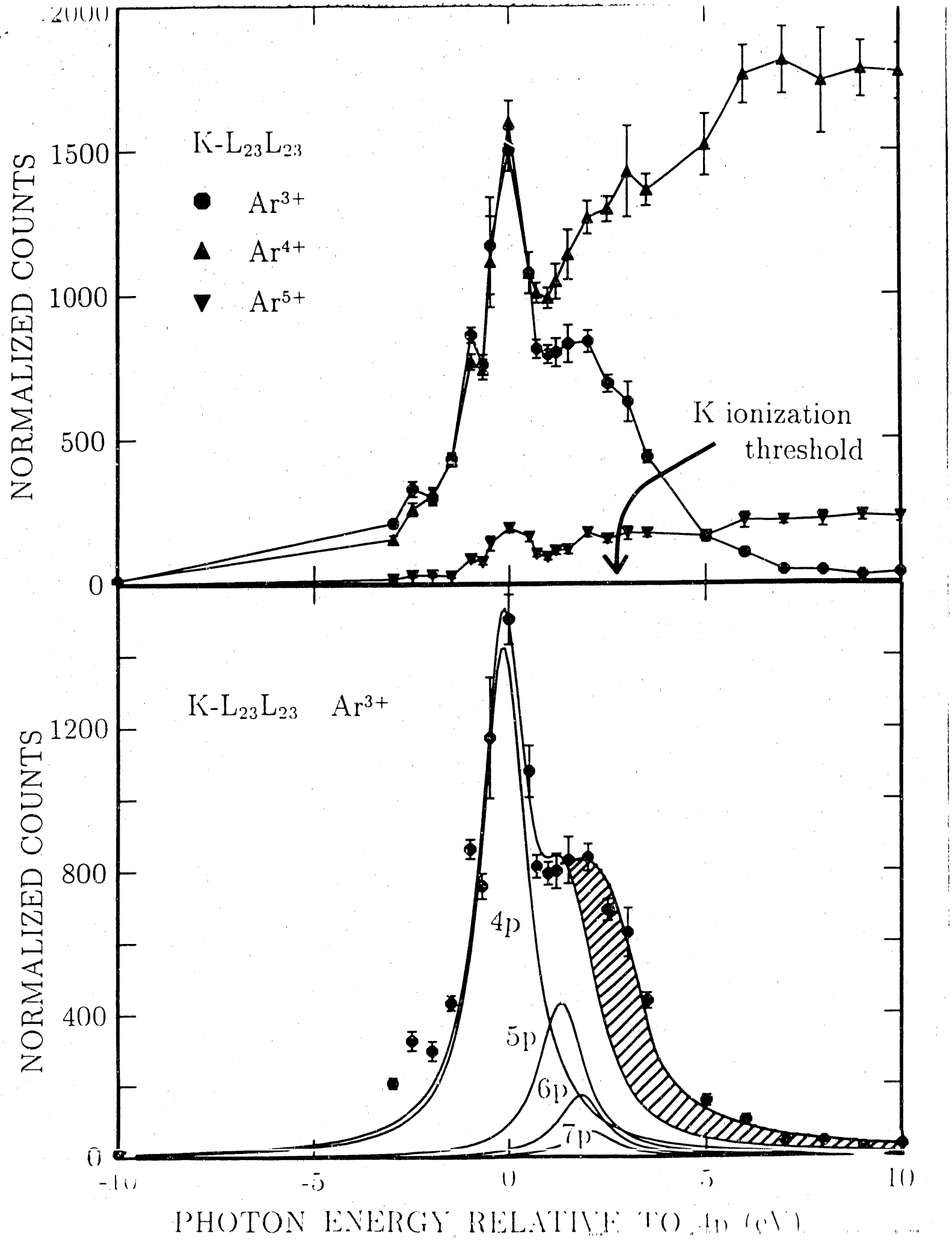
2000
1500
1000
500
0
NORMALIZED COUNTS
K-L23L23
Ar3+
Ar4+
Ar5+
K ionization
threshold
1200
800
400
0
NORMALIZED COUNTS
K-L23L23 Ar3+
4p
5p
6p
7p
-10
-5
0
5
10
PHOTON ENERGY RELATIVE TO 4p (eV)

END

DATE FILMED

11 / 07 / 90